Cation incorporation into biochar affects alkalinity-driven carbon dioxide removal accounting

*Ayesha A. Ahmed[1], Tim Jesper Suhrhoff[2,1], Christopher T. Reinhard[3], Noah J. Planavsky[1,2]

[1]Department of Earth and Planetary Sciences, Yale University, New Haven, CT 06511; [2]Yale Center for Natural Carbon Capture, New Haven, CT 06511; [3]School of Earth and Atmospheric Sciences, Georgia Institute of Technology, Atlanta, GA 30332.

*Corresponding author: ayesha.a.ahmed@yale.edu

Abstract

Biochar production from biomass may be a scalable and cost-effective means of atmospheric carbon dioxide removal. Current accounting frameworks, however, focus primarily on persistent organic carbon and overlook how pyrolysis alters the return of biomass-derived ions to soils and waters. Here, we quantify a first-order alkalinity-related adjustment to biochar CDR by comparing the inorganic carbon cycling implications of biochar production with a biomass-decay counterfactual. During plant growth, net cation uptake generates soil acidity, which can consume bicarbonate alkalinity and shift the carbonate system toward dissolved CO_2, causing CO_2 emissions upon re-equilibration with the atmosphere. Biomass decay can eventually reverse this acid-base perturbation by returning cations to the biogeochemical cycle. Biochar formation delays or prevents part of this return flux by retaining cations and anions within the biochar matrix, making permanent or prolonging what would otherwise have been a temporary CO_2 source. We estimate the resulting change in inorganic carbon cycling from the cation–anion charge equivalent imbalance associated with the retained elemental inventory relative to recalcitrant organic-carbon storage. Across observations reporting complete Ca, Mg, K, Na, N, and S data (n = 85), the mean alkalinity-related reduction in effective CDR is 3.2%

when the retained elemental inventory is assumed to be released in proportion to biochar degradation. If cations and anions are instead retained preferentially as organic carbon is lost, the mean reduction increases to 3.9% and 5.1% when 82% and 63% of organic carbon persists, respectively. The fraction of observations showing a reduction in effective CDR of ≥5% similarly increases from 18.8% under proportional release to 21.2% and 22.4% under the two complete element retention scenarios. Individual biochars span a wide range of compositions and durabilities through time, including cases in which the inorganic carbon effect instead increases estimated net CDR.

Keywords

Biochar; Carbon Dioxide Removal; Monitoring, Reporting, and Verification (MRV); Inorganic Carbon Cycling; Cation Retention

1 INTRODUCTION

Carbon dioxide removal (CDR) is viewed as an essential part of meeting international climate goals (IPCC, 2023; Lehmann et al., 2021). Most pathways that keep peak climate warming below 2°C will require a dramatic and rapid increase in CDR deployment in the coming decades as a supplement to aggressive decarbonization (IPCC, 2023; Lehmann et al., 2021). Although there is an increasing focus on government procurement programs, to date most CDR projects have been developed and funded through voluntary carbon markets (VCMs). However, there have recently been a series of articles strongly critiquing the efficacy of VCMs. Projects aiming to scale organic carbon storage (e.g., forest and soil management) have proven particularly contentious (Wu et al., 2023). In step with a reevaluation of the efficacy of VCMs and a crash in prices for carbon credits, there have been more vocal calls for investment in "durable" CDR - pathways for which carbon is removed for timescales of at least hundreds of years. There has been a particular focus on the production of biochar (Lefebvre et al., 2023; Lehmann et al., 2021), the persistent form of solid, carbonaceous residue of anoxically pyrolyzed organic matter.

Biochar projects can be implemented in most working lands and potentially deployed at scale. For instance, it has been proposed that biochar has the potential to account for 3 gigatons (Gt = 10^9 tons) of CDR annually, out of roughly 5-10 Gt/year of CDR necessary by 2050 to meet climate goals (IPCC, 2023). Assuming a nominal price of $100 per ton of biochar derived CDR, this process could rapidly become a >$100 billion dollar/year industry. As CDR marketplaces grow, there has been a proliferation of companies aiming to remove carbon via biochar application to soil. These companies strive to commercially produce biochar as an affordable and effective soil amendment in a wide range of agricultural settings. Currently, there are more than 250 biochar suppliers listed on the largest CDR supplier database, and as of May 2026, these companies have pledged to remove ~16 million tons of carbon dioxide via biochar with more than 1.4 million tons of CDR having already been delivered *(CDR.Fyi*, 2026). Furthermore, biochar CDR sales increased nearly three orders of magnitude between 2020 through 2025 (*CDR.Fyi*, 2026).

Existing CDR crediting protocols frame biochar as a CDR strategy based upon the comparison of two scenarios. In the first scenario, biomass waste is pyrolyzed to produce biochar and amended to soil as an alternative to disposal, meaning organic carbon is transformed into stable, recalcitrant structures and stored over the long term in a soil environment. In the second (counterfactual) scenario, biomass waste is left to decompose back into the soil as a method of disposal or otherwise lost (e.g., via burning) and the organic carbon is released back into the environment. With respect to biogeochemical storage in soil, this comparison is therefore centered primarily on the fate and persistence of organic carbon, alongside the life-cycle emissions associated with biochar production and deployment (Etter et al., 2025; Schimmelpfennig & Glaser, 2012).

Biomass growth and decay also involve the cycling of inorganic nutrients that affect soil acid–base balance (H. Marschner, 2011; Tang & Rengel, 2003). In particular, net cation uptake generates soil acidity, which can be reversed when biomass decomposes and associated net cation charge equivalents are returned to the soil. By stabilizing biomass and retaining part of its elemental inventory, biochar can delay or prevent this reversal and thereby preserve an alkalinity deficit that would otherwise be transient. Because acidity release can promote CO_2 release upon carbonate-system re-equilibration, biochar production may impose an inorganic carbon-removal penalty alongside its primary organic-carbon storage benefit. Here, we quantify this first-order alkalinity-related adjustment of carbon storage and compare its magnitude with the durable organic-carbon storage conventionally credited to biochar.

1.1 Plant cation cycling and soil acidification

Plants acquire mineral nutrients from the soil solution, many of which are taken up as positively or negatively charged ions. Major nutrient cations include K^+, Ca^{2+}, and Mg^{2+}, while important nutrient anions include NO_3^-, $H_2PO_4^-/HPO_4^{2-}$, and SO_4^{2-} (H. Marschner, 2011). Depending on metabolic and structural needs, living plants, including crops, maintain charge balance within their tissue by absorbing and releasing cations and anions

(Cunningham, 1964; de Wit et al., 1963). These species become constituent parts of the biomass.

Net cation uptake—the uptake of more positive than negative charge—is compensated by the release of charge-equivalent protons from roots, whereas net anion uptake is accompanied by proton uptake and/or release of base equivalents (Hinsinger et al., 2003; Tang & Rengel, 2003). Plants commonly take up more cation than anion charge during growth, making net cation uptake a well-established source of rhizosphere and soil acidification (de Wit et al., 1963; Hinsinger et al., 2003; Tang & Rengel, 2003). In agricultural systems, this process contributes to long-term soil acidification, particularly where biomass containing excess cation charge is removed through harvest rather than returned to the soil (Tang & Rengel, 2003).

However, in the biomass-decay counterfactual considered here this growth-associated acidification is not necessarily permanent. Decomposition returns the elemental and acid-base inventory stored in plant material to the soil system, and incorporation of plant residues with high excess-cation or ash alkalinity can increase soil pH as these base equivalents are released (Sparling et al., 1999; Tang & Rengel, 2003). Thus, for the first-order growth–decay cycle considered here, decomposition of biomass tends to reverse the acid-base perturbation associated with plant growth.

1.2 Effect of biochar pyrolysis on carbon and elemental storage

Biochar is produced by pyrolyzing biomass, an anoxic thermochemical process that converts part of biomass carbon into persistent structures resistant to oxidation and degradation (Joseph et al., 2021). This stabilization of biomass-derived carbon is biochar's primary CDR function, extending carbon residence times in soil far beyond those of the original biomass (Lefebvre et al., 2023; Lehmann et al., 2021). Biochar can also affect soil fertility, pH, water retention, greenhouse-gas emissions, and soil organic-matter dynamics, although these broader effects are not the focus here (Huang et al., 2023; Joseph et al., 2021; Lehmann et al., 2021; Van Zwieten et al., 2015; J. Wang et al., 2016).

Pyrolysis also transforms and redistributes the biomass elemental inventory. Cations (e.g., Na, K, Ca, Mg) and anions or anion-forming elements (e.g., N, S, P, Cl) can remain embedded in biochar in organometallic complexes, oxides, carbonates, carbonaceous structures, or micropores, depending on feedstock and pyrolysis conditions (Buss et al., 2022; Joseph et al., 2021; Nan et al., 2021; Xu et al., 2017). These mineral- and cation-associated phases contribute to carbon retention and biochar stability (Buss et al., 2022; Nan et al., 2021). In contrast, exchangeable ions are transiently sorbed to charged surfaces and remain responsive to surrounding porewater chemistry (Joseph et al., 2021). Analytical protocols may remove this exchangeable pool by leaching or extraction before quantifying the more strongly retained elemental inventory considered here. The non-extractable and non-leachable ions are the subject of this study.

Relative to biomass decomposition, pyrolysis therefore alters two coupled return fluxes: organic carbon and the biomass elemental inventory. Some biomass constituents are volatilized or partitioned into ash, whereas others remain in the biochar. Nitrogen, for example, can be lost as N_2O or NO_x during pyrolysis or quenching (S. Li, 2024), while plant-derived cations can be preferentially retained. Consequently, the retained cation-to-anion charge ratio can vary among biochars as a function of feedstock composition and pyrolysis conditions (Buss et al., 2022; Joseph et al., 2021; Nan et al., 2021).

1.3 Inorganic CDR implications of biochar generation

The effects of biomass growth and degradation on soil acid–base balance also have consequences for inorganic carbon cycling. In bicarbonate-bearing soils and waters, acidity consumes carbonate alkalinity and shifts carbonate-system speciation toward dissolved CO_2:

$$CO_2(g) + H_2O\ (l) \rightleftharpoons H_2CO_3\ (aq) \rightleftharpoons HCO_3^-(aq) + H^+(aq)$$

Addition of acidity therefore shifts this equilibrium toward the left, titrating bicarbonate to CO_2:

$$H^+ + HCO_3^- \rightarrow CO_2 + H_2O$$

and can ultimately lead to CO_2 evasion as the aqueous system re-equilibrates with the atmosphere. This response does not need to occur where protons are released: acidity can be buffered or transported through soils and hydrological networks before encountering bicarbonate-rich waters, so carbonate-system re-equilibration may occur locally or downstream (DeVries, 2022; Drever, 1988; Zeebe & Wolf-Gladrow, 2001). Over a given carbon accounting horizon, biochar production can therefore delay or prevent reversal of an acidity effect that would otherwise tend to be transient during a complete biomass growth–decay cycle. Although biochar cation and anion storage and charge balance in soil waters are well-established concepts (Buss et al., 2022; Drever, 1988; Nan et al., 2021; Xu et al., 2017; Zeebe & Wolf-Gladrow, 2001), to our knowledge their implications for alkalinity-related biochar CDR accounting have not been quantified. An analogous charge-equivalent framework is widely used for enhanced weathering, where alkalinity generated by mineral dissolution contributes to CDR while acidity inputs consume alkalinity and reduce creditable removal (Beerling et al., 2020; Clarkson et al., 2024; Suhrhoff et al., 2026).

Here, we apply a first-order inorganic carbon-accounting framework to biochar by comparing biochar production with a biomass-decay counterfactual while holding other background acid–base inputs constant. Our quantitative estimates therefore apply specifically to biomass decay as the counterfactual considered here; actual biochar projects may involve alternative biomass fates, for which the magnitude and timing of the adjustment would require project-specific evaluation. We term the resulting difference the "alkalinity-driven CDR adjustment" and compare it with durable organic-carbon storage. Using a novel database pairing biochar carbon content with incorporated cation and anion

194 concentrations, we quantify the magnitude and variability of this adjustment arising from
195 the net elemental charge retained in biochar over the accounting horizon.

2. MATERIALS AND METHODS

2.1 Biochar database and elemental data

Based on a literature review of diverse types of biochar (see data SI), we collected information about elemental composition of base cations (i.e. Ca^{2+}, Mg^{2+}, K^{+}, Na^{+}), anions (i.e. N and S when provided), and the biochar's percent organic carbon. Manure- and animal-litter-derived biochars were retained in the dataset. For these feedstocks, we assume that the measured cation–anion imbalance predominantly reflects elements originally incorporated into biomass and subsequently transferred through animal feed, such that the same biomass-growth–decay acid–base framework can be applied. Elemental concentrations were converted to molar concentrations and then to charge equivalents according to the valence assigned to each element. Biochar's cation concentrations in the database are from studies that first leached out the exchangeable fraction of cations and then carried out elemental analysis of the biochar. Elemental concentrations were derived from either X-ray fluorescence (XRF) analysis or elemental analysis following acid digestion (Abdel-Fattah et al., 2015; Alburquerque et al., 2016; Al-Rabaiai et al., 2024; Altıkat et al., 2024; Al-Wabel et al., 2013; Anđelini et al., 2023; Anjum et al., 2014; Boraah et al., 2023; Brantley et al., 2016; Butnan et al., 2015; Cantrell et al., 2012; Drané et al., 2024; Enders et al., 2012; Fernández et al., 2014; Jia et al., 2012; Katuwal et al., 2022; Kwoczynski et al., 2024; Lataf et al., 2022; S. Li & Shangguan, 2018; Macdonald et al., 2014; Mohanty et al., 2013; Naeem et al., 2014; Novak et al., 2013; Noyce et al., 2017; Nwajiaku et al., 2018; Obey et al., 2022; Omotade et al., 2020; Singh et al., 2010; Subedi et al., 2016; Tepecik et al., 2024; Usman et al., 2015; K. Wang et al., 2020; Y. Wang et al., 2013; Williams & Thomas, 2023; Wrobel-Tobiszewska et al., 2015; Xiao et al., 2018; Yang et al., 2023; Zhang et al., 2020; Zhao et al., 2018). Because the charge-equivalent calculation is based on total elemental inventories rather than the molecular species present after pyrolysis, post-pyrolysis molecular speciation was not used in the calculation. Acid digestion provides total elemental concentrations irrespective of molecular speciation, while XRF similarly quantifies elemental composition of the analyzed solid. We restricted the literature compilation to studies published from 2005 onward; this criterion had little effect on database size because most biochar characterization studies were published after this date.

Following Woolf et al. (2021), pyrolysis products containing less than 10 wt.% organic carbon were excluded from the database.

2.2 Net cation uptake impact on CDR

Excess cation charge of biochar was calculated by subtracting anionic charge (nitrogen, sulfur) from cationic charge (calcium, magnesium, potassium, sodium):

$$Q_{net} = 2n_{Ca} + 2n_{Mg} + n_K + n_{Na} - n_N - 2n_S$$

where n_x is the molar concentration of element x in the biochar (mol kg^{-1} biochar), and Q_{net} is expressed as mol charge equivalents kg^{-1} biochar. Importantly, Q_{net} does not represent a net electrical charge of the biomass or biochar. Rather, it represents the net ionic charge imbalance associated with uptake of the quantified cations and anions from soil porewaters during plant growth. Electroneutrality is maintained during uptake through compensating processes, including proton release or uptake by roots (de Wit et al., 1963; Hinsinger et al., 2003; Tang & Rengel, 2003) ; thus, Q_{net} is an acid–base accounting balance calculated from the measured elemental inventory under the ionic-equivalent assumptions specified below and is used as a first-order proxy for the net ionic imbalance associated with biomass nutrient uptake and return. Positive values indicate an excess of retained cation charge, whereas negative values indicate an excess of retained anion-equivalent charge.

For this first-order accounting, Ca, Mg, K, and Na are treated as Ca^{2+}, Mg^{2+}, K^+, and Na^+, respectively. Total reported N and S are assigned nitrate- and sulfate-equivalent charge in the biomass-decay counterfactual, corresponding to one negative charge equivalent per mole of N and two negative charge equivalents per mole of S. This represents an end-member acid–base accounting assumption regarding the forms in which biomass-derived N and S ultimately enter the aqueous biogeochemical cycle, rather than an assumption about their molecular forms within biochar which is not relevant to this analysis. Subsequent processes—including nitrogen transformations, nutrient re-uptake and

leaching, cation exchange processes, and mineral precipitation and dissolution (Calabrese et al., 2022; Jahanzad et al., 2016; Redin et al., 2014; Suhrhoff et al., 2026)—can generate or consume acidity and therefore modify the ultimate inorganic carbon response but are not assessed here.

Chlorine, a plant micronutrient (Broadley et al., 2012), and phosphorus were excluded from the database because both are inconsistently reported in the biochar elemental-composition literature. Because Cl and P are not represented, calculated net cation charge may be biased positive where these elements contribute materially to the retained anion-equivalent inventory; the available dataset does not permit the magnitude of this potential bias to be quantified systematically, but since these are minor components of biomass (H. Marschner, 2011) we expect the impact of this accounting choice to be low.

The measured Q_{net} describes the initial cation-anion equivalent imbalance associated with the reported elemental inventory of the biochar. To account explicitly for release of this inventory as biochar mineralizes, we define r_{ion} as the fraction of the initial equivalent imbalance released back to the biogeochemical cycle over the 100-year accounting horizon, and f_{ion} as the fraction that remains withheld in the biochar-associated pool:

$$f_{ion} = 1 - r_{ion}$$

The fraction of the initial equivalent charge imbalance that is withheld was converted to an equivalent alkalinity-related CO_2 adjustment. For this first-order calculation, consistent with standard accounting in enhanced weathering CDR quantification (Clarkson et al., 2024; Suhrhoff et al., 2026) and the carbonate-system assumption described in Section 1.3, one mole of retained excess cation equivalents was treated as one equivalent of foregone alkalinity export due to plant-based soil acidification and approximated as one mole of foregone CO_2 removal. The alkalinity-related CO_2 adjustment remaining at the accounting horizon was therefore calculated as:

$$\Delta CO_{2,alk} = Q_{net} \times f_{ion} \times M_{CO_2}$$

where M_{CO_2} = 44.009 g mol^{-1}. Positive values represent foregone CO_2 removal relative to the biomass-decay counterfactual, whereas negative values represent an increase in calculated CO_2 removal. This formulation separates the initial elemental equivalent imbalance from the fraction of that imbalance that remains withheld over the accounting horizon.

2.3 Organic-carbon persistence and overall adjustment of biochar CDR

The overall effect of the alkalinity-driven adjustment on net biochar CDR depends on the persistence of both components of the accounting: the net elemental charge retained over the accounting horizon and the fraction of organic carbon that remains unmineralized. The relative adjustment is therefore controlled by the amount of persistent net elemental charge per unit of persistent organic carbon. To quantify the latter, we calculated durable organic-CDR from the measured organic-carbon content and the fraction assumed to remain unmineralized over 100 years. Following Woolf et al. (2021), we evaluated two end-member persistence assumptions: 63% (low recalcitrance) and 82% (high recalcitrance). We denote this organic-carbon persistence fraction as f_{rec}. For each biochar, we estimate $CO_{2,org}$ as:

$$CO_{2,org} = 10 \times C_{org} \times f_{rec} \times (M_{CO_2}/M_C)$$

where C_{org} is the measured organic-carbon content of the biochar (wt.%), f_{rec} is either 0.63 or 0.82 (Woolf et al., 2021), and M_C = 12.011 g mol^{-1}. The resulting CO_{2org} is expressed as grams of CO_2-equivalent durably stored per kilogram of biochar. The alkalinity-related CDR adjustment (A_{CDR}) was then expressed relative to durable organic-carbon storage. Substituting the expressions above makes explicit that the relative adjustment depends on the net elemental charge-to-organic-carbon ratio, scaled by their respective persistence fractions:

$$A_{CDR}[\%] = 100 \times \frac{\Delta CO_{2,alk}}{CO_{2,org}} = 100 \times \frac{Q_{net} \times M_C}{10 \times C_{org}} \times \frac{f_{ion}}{f_{rec}}$$

Accordingly, a positive percentage represents a reduction in net CDR relative to organic-carbon storage alone, whereas a negative value represents an increase in calculated CDR under the first-order accounting assumptions, representing an excess of anion charge compared to cation content.

2.4 Biochar degradation scenarios

Long-term constraints on the relative release rates of biochar organic carbon and matrix-associated elemental inventories are limited. We therefore evaluate three bracketing persistence scenarios. In the first, proportional-release scenario, release of the cation-anion equivalent imbalance scales proportionally with organic carbon loss from biochar degradation, such that $r_{ion} = 1 - f_{rec}$ and therefore $f_{ion} = f_{rec}$. Under this assumption, the persistence fractions cancel from the relative CDR adjustment:

$$f_{ion} = f_{rec} \Rightarrow A_{CDR} = 100 \times \frac{Q_{net} \times M_C}{10 \times C_{org}}$$

Consequently, the proportional-release scenario gives the same relative alkalinity-related CDR adjustment for $\underline{f_{rec}} = 0.63$ and $\underline{f_{rec}} = 0.82$, although the absolute amounts of durable organic-carbon storage and the remaining alkalinity-related CO_2 adjustment both scale with $\underline{f_{rec}}$.

There is a mechanistic basis to consider proportional release a conservative lower-bound assumption for the magnitude of the relative adjustment. Mineral cations and mineral-associated phases can participate in organometallic associations, protective phases, and other structures that enhance carbon retention and biochar stability (Buss et al., 2022; Joseph et al., 2021; Nan et al., 2021; Xu et al., 2017). Because cations may contribute to

biochar stability through cation bridging, carbon that is less strongly stabilized by these interactions may be preferentially degraded, leading to preferential retention of cations in the residual biochar. Hence, we evaluate two additional scenarios that together with the proportional release scenario bracket the plausible range of biochar degradation processes in which $f_{ion} = 1$ over 100 years while organic carbon persists at either $f_{rec} = 0.63$ or $f_{rec} = 0.82$ (see Table 1).

Table 1: Organic-carbon and elemental-retention scenarios used to calculate the alkalinity-related CDR adjustment

Scenario	f_{rec}	f_{ion}	f_{ion} / f_{rec}	**Interpretation**
Proportional release	0.63 or 0.82	$f_{ion} = f_{rec}$	1.00	Elemental equivalent imbalance is released in direct proportion to organic-C loss; relative adjustment is independent of f_{rec}.
Complete elemental retention; low C persistence	0.63	1.00	1.59	All measured equivalent imbalance remains withheld while 63% of organic C persists.
Complete elemental retention; high C persistence	0.82	1.00	1.22	All measured equivalent imbalance remains withheld while 82% of organic C persists.

Primary summary statistics were calculated for observations reporting Ca, Mg, K, Na, N, and S together ($n = 85$). This complete-element subset minimizes directional bias from omission of individual represented ion pools and is therefore used for the main estimates under each persistence scenario. To characterize the sensitivity of inferred adjustments to the incomplete elemental reporting common in the source literature, we additionally analyzed three broader datasets: (i) all observations using whatever subset of Ca, Mg, K, Na, N, and S was reported for each biochar ($n = 215$); (ii) observations reporting both N and S, with the cation-equivalent balance calculated from whichever of Ca, Mg, K, and Na were reported ($n = 121$); and (iii) observations reporting N, with the cation-equivalent balance calculated from whichever of Ca, Mg, K, and Na were reported ($n = 194$ Summary values are reported as means ± sample standard deviations and medians. To evaluate sensitivity to unequal representation among source studies, observations in the complete-element primary subset were additionally averaged within study before summarizing across the represented studies. Analytical measurement uncertainty was not propagated

368 because measurement uncertainties are not reported consistently across the source
369 literature.

3. RESULTS

Our analysis suggests that net cation incorporation during biochar production can have a non-negligible effect on the overall CDR associated with biochar amendment to soil. Our database comprises 215 biochar observations drawn from 39 source publications, some of which are review papers compiling data from additional studies. Our primary analysis was restricted to the 85 observations reporting Ca, Mg, K, Na, N, and S together, representing eight source studies. Under the proportional-release scenario ($f_{ion} = f_{rec}$), the mean A_{CDR} was 3.2% ± 7.4%, with a median of 0.74% and a range from −7.8% to 39.1% (Fig. 1). Assuming complete retention of the measured cation–anion imbalance over the accounting horizon ($f_{ion} = 1$) increased the mean A_{CDR} to 3.9% ± 9.0% at $f_{rec} = 0.82$ and 5.1% ± 11.7% at $f_{rec} = 0.63$, with corresponding medians of 0.91% and 1.18% and ranges of −9.5% to 47.7% and −12.3% to 62.1%, respectively (Fig. 1). The proportion of observations with $A_{CDR} \geq 5\%$ was 18.8%, 21.2%, and 22.4% under proportional release, complete elemental retention with $f_{rec} = 0.82$, and complete elemental retention with $f_{rec} = 0.63$, respectively (Fig. 2a).

For a specific example, a grapevine-residue biochar containing 77.2% organic carbon contained 17.38 mol of base-cation charge and 1.67 mol of anion-equivalent charge per kilogram of biochar, giving $Q_{net} = 15.71$ mol charge equivalents kg^{-1}. This corresponds to an initial alkalinity-related CO_2 adjustment of 691 gCO_2 eq kg^{-1} biochar. At $f_{rec} = 0.82$ and 0.63, durable organic-carbon storage is 2,319 and 1,782 gCO_2 eq kg^{-1} biochar, respectively. Under proportional release, the remaining alkalinity-related CO_2 adjustment scales to 567 and 436 gCO_2 eq kg^{-1}, yielding the same relative A_{CDR} of 24.4% at both persistence assumptions. If the measured elemental imbalance is instead completely retained ($f_{ion} = 1$), the full 691 gCO_2 eq kg^{-1} remains withheld, increasing A_{CDR} to 29.8% at $f_{rec} = 0.82$ and 38.8% at $f_{rec} = 0.63$. In contrast, a eucalyptus-wood biochar containing 69.7% organic carbon contained 0.67 mol of base-cation charge and 0.17 mol of anion-equivalent charge per kilogram, giving $Q_{net} = 0.50$ mol charge equivalents kg^{-1} and an initial alkalinity-related adjustment of only 22.1 gCO_2 eq kg^{-1}. Its A_{CDR} is consequently 0.87% under

proportional release and 1.06% and 1.37% under complete elemental retention at f_{rec} = 0.82 and 0.63, respectively.

A biochar with a negative A_{CDR} contains more assigned anion-equivalent charge than base-cation charge and, under the first-order accounting assumptions used here, would therefore increase calculated CDR relative to accounting based on recalcitrant organic carbon alone. Within the complete six-element subset, 25 of 85 observations (29.4%) had negative A_{CDR}. Because the three persistence scenarios scale the same underlying cation–anion balance without changing its sign, this fraction is identical among scenarios. Only two observations (2.4%) had $A_{CDR} < -5\%$ in each of the three scenarios, whereas the positive tail extended to 39.1%, 47.7%, and 62.1% under proportional release and the two complete-element-retention scenarios, respectively (Figs. 1–2).

The estimated magnitude and distribution of A_{CDR} were sensitive to elemental-data completeness (Figs. 2–3). When all 215 observations were analyzed using whatever subset of Ca, Mg, K, Na, N, and S was reported for each biochar, mean A_{CDR} values were 3.8 ± 7.2%, 4.6 ± 8.8%, and 6.0 ± 11.5% under proportional release, complete elemental retention with f_{rec} = 0.82, and complete elemental retention with f_{rec} = 0.63, respectively; corresponding medians were 1.18%, 1.44%, 1.88%. In this available-element analysis, 26.0%, 30.2%, 34.0% of observations had $A_{CDR} \geq 5\%$, compared with 18.8%, 21.2%, and 22.4% in the complete six-element subset (Fig. 2). The N+S subset, in which Q_{net} was calculated from whichever cations were reported (n = 121), yielded lower mean A_{CDR} values of 2.52%, 3.07%, 4.00%, whereas observations reporting N together with any reported cations (n = 194) yielded means of 3.69%, 4.51%, 5.86% for the same three persistence scenarios (Fig. 3).

Our primary analysis is conducted at the individual-biochar level because multiple observations reported within a single study generally represent distinct biochars, feedstocks, pyrolysis conditions, or experimental treatments and therefore contain genuinely different compositional information. To nevertheless evaluate sensitivity to

unequal representation among source studies, we additionally averaged the complete six-element observations within study before summarizing across the eight represented studies. Study-level mean A_{CDR} values were 3.5% ± 8.5% under proportional release, 4.3% ± 10.4% under complete elemental retention with f_{rec} = 0.82, and 5.6% ± 13.5% under complete elemental retention with f_{rec} = 0.63, with corresponding medians of 1.98%, 2.41%, and 3.14%. Study-level means ranged from −7.6% to 21.7%, −9.3% to 26.4%, and −12.0% to 34.4%, respectively. In each scenario, two of eight studies (25%) had a mean $A_{CDR} \geq 5\%$. The study-level analysis therefore retains the broad variability and positive mean adjustment observed at the row level, indicating that the result is not solely driven by studies contributing large numbers of observations.

4. DISCUSSION

4.1 Magnitude, persistence, and reversibility of the alkalinity-related CDR adjustment

We present a data compilation and a simple framework to demonstrate that consideration of cation and anion incorporation into biochar can affect biochar CDR estimates when inorganic carbon cycling is considered alongside persistent organic-carbon storage. The compilation allows us to provide an initial, first order, assessment of the impact of net cation incorporation in biochar on CDR accounting over the 100-year persistence horizon considered here. Our results indicate that excluding this inorganic contribution can lead to either over- or under-estimation of CDR relative to accounting based on persistent organic carbon alone, depending on the net retained charge. However, the consistently positive mean adjustment across persistence scenarios suggests that current biochar CDR accounting approaches that omit this effect are, on average, likely to slightly overestimate net CDR.

The consistency between row- and study-level estimates indicates that the central result is not driven solely by studies contributing large numbers of observations. The differences among our three scenarios highlight that the alkalinity-related CDR adjustment depends on the relative persistence of organic carbon and the relative rate at which the associated elemental inventory is released. In this context, the relative extent to which cations are released upon biochar degradation is an important area of future research. While analyses based on more limited elemental reporting allow us to utilize a larger fraction of the existing data with findings generally showing similar tendencies between subsets, the differences among these estimates also demonstrate that more complete reporting of biochar cation and anion inventories would be valuable in future studies.

A process not explored here is long-term (>100 years) aging of the recalcitrant biochar matrix, which may eventually return part of the stored carbon and elemental inventory to the biogeochemical cycle. The alkalinity-related adjustment may therefore partly or fully reverse if retained cations and anions are released beyond the accounting horizon,

representing a delay rather than a permanent reduction in CDR over the full lifetime of the biochar. However, this timing remains relevant (Cabiyo et al., 2026). In the biomass-decay counterfactual, decomposition returns net cation charge and associated base equivalents, allowing recovery of the growth-associated alkalinity deficit within the shorter timescale of plant growth and decomposition. Delaying this return of net cation change and associated base equivalents through biochar formation correspondingly delays that alkalinity recovery and associated CO_2 removal to a future, higher-CO_2 atmosphere, lowering the overall climate benefit of biochar at the time of biochar production. Thus, even where the adjustment is ultimately reversible, its timing affects the climate benefit and time-bounded accounting of biochar CDR.

An additional process that may influence inorganic carbon cycling is the evolution of biochar surface charge during aging. As biochar surfaces oxidize, new cation-exchange sites can develop, altering cation retention and associated acid–base dynamics (H. Li et al., 2019; L. Wang et al., 2020). Increased adsorption of base cations at newly developed exchange sites (Qadir et al., 2024) could further modify the alkalinity-related CDR adjustment because, where these sites are initially protonated, their deprotonation and subsequent occupation by base cations can release H^+ to soil solution. This represents an additional source of acidity distinct from the delayed return of biomass-derived net cation charge quantified here and could therefore increase the magnitude of the alkalinity-related adjustment. Conversely, cation desorption from exchange sites would also affect base-cation mobility and associated alkalinity dynamics. The magnitude of these effects will depend on the development and protonation state of exchange sites, soil pH, cation availability, and the degree of cation saturation during biochar aging, and is not quantified in our present framework.

4.2 Additional processes modifying the first-order alkalinity adjustment

Beyond the relative persistence of organic carbon, the retained elemental inventory, and aging-dependent changes to biochar surface chemistry considered above, several additional biogeochemical processes could modify the magnitude or even the direction of the first-

order alkalinity-related CDR adjustment. These processes act either on the subsequent fate of the released elemental inventory or through broader changes to nutrient cycling and requirements, soil buffering, and mineral reactions following biochar deployment.

While cations can form secondary phases upon release or be lost to cation exchange (Calabrese et al., 2022; Kanzaki et al., 2025) and N can undergo subsequent transformations such as denitrification (Chiaravalloti et al., 2023), timescales of elemental release upon biochar degradation and post-release processes modulating these remain poorly constrained. Nevertheless, these processes can substantially alter the fate, timing, and ultimate impacts of the associated alkalinity perturbation during transport through soils and waters. Additionally, total elemental N also does not constrain either the ionic form through which N was acquired during plant growth or the form in which it is returned during decomposition. Because nitrate carries negative charge, treating all measured N as nitrate-equivalent represents a deliberately conservative choice with respect to the net-cation signal quantified here. Uptake as ammonium or neutral organic N would increase the inferred net cation-equivalent imbalance and, all else equal, strengthen the alkalinity related downward adjustment of net CDR. We do not attempt to account for subsequent N cycling following biomass decomposition, including ammonification, nitrification, denitrification, or biological re-uptake, and their associated effects on acidity and alkalinity (Bolan et al., 1991). Rather, our framework isolates the direct first-order consequence of stabilizing biomass and thereby altering the return of its elemental acid–base inventory relative to biomass decomposition.

A further consequence of diverting biomass from decomposition to biochar production is delayed or reduced nutrient recycling. If biomass that would otherwise decompose is converted to persistent biochar, part of its N and P inventory may be withheld from near-term return to soil, potentially increasing external nutrient requirements where these inputs are needed to maintain fertility and productivity. Any resulting increase in mineral-fertilizer demand would constitute an additional life-cycle carbon cost relative to decomposition (Menegat et al., 2022; Walling & Vaneeckhaute, 2020). Biochar also affects

N and P cycling through numerous other processes whose magnitude and direction depend on feedstock, pyrolysis conditions, soil properties, and time since application (Gao et al., 2019; Gul & Whalen, 2016). We do not quantify these effects here, but they represent an additional life-cycle consequence of the biochar versus biomass decay counterfactual that would further reduce net project level CDR.

As biochar CDR projects scale up and expand to a wider range of settings, such as highly acidic (Waheed et al., 2026), calcareous, arid, or submerged soils, biochar's net cation incorporation will interact with soil-specific buffering and transport processes, depending not only on the biomass feedstock and pyrolysis conditions as explained earlier, but also on soil pH, mineralogy, exchange capacity, hydrology, and background alkalinity. The impact of soil variability on the alkalinity-related CDR adjustment and its fate considering downstream processes is an important area for future soil science and aqueous geochemistry research. Dissolution of biochar-associated ash and mineral phases can also return retained base cations to the biogeochemical cycle. To the extent that this represents release of the biomass-derived net cation inventory quantified here, it constitutes a reversal of the alkalinity-related adjustment and is represented at first order by our elemental-release scenarios, including the proportional-release case. However, ash dissolution may also generate alkalinity through mineral phases or processes not captured by the retained cation–anion balance, which could further modify net CDR. Stacking biochar and enhanced weathering as a means of CDR (Buss et al., 2021; Sohng et al., 2025; Meyer zu Drewer et al., 2026) has also been proposed and tested experimentally, further emphasizing the need to resolve interacting organic and inorganic carbon fluxes.

5. CONCLUSION

Biochar CDR is typically quantified primarily from persistent organic-carbon storage, together with project-level life-cycle emissions and permanence considerations. Our results show that changes to inorganic carbon cycling can introduce an additional, and in some cases material, adjustment to net CDR that mostly reflects a net reduction in CDR. The magnitude of this effect depends on biochar composition, the relative persistence of organic carbon and retained elemental inventories, and the biogeochemical context in which biochar is deployed. Where this adjustment is material, it therefore has direct implications for how much CDR can defensibly be attributed to a biochar project and, consequently, how that removal is quantified and credited.

This is particularly relevant because biochar projects are increasingly evaluated through carbon-crediting methodologies on the VCM that translate project-level carbon accounting into issued CDR credits. Current verification frameworks used by platforms such as Verra, Isometric, and Puro account for greenhouse-gas emissions associated with feedstock transport, biochar production, transport, and application, as well as changes in CDR permanence as biochar ages (Etter et al., 2025; Schimmelpfennig & Glaser, 2012). However, to our knowledge current biochar verification methodologies do not explicitly account for the fate of incorporated net cations and the associated alkalinity-related CDR adjustment. The life cycle assessment of these projects may be robust, but this potentially represents an omitted geochemical term in carbon accounting (Nordahl et al., 2024). If the alkalinity-driven adjustment identified here is material under a project's specific feedstock, soil conditions, and counterfactual, omitting it could bias estimates of net CDR and associated crediting. However, the magnitude of this effect will likely vary considerably between projects.

Therefore, we suggest that biochar CDR quantification frameworks should consider the geochemical impacts of net cation incorporation into the biochar matrix and associated inorganic carbon cycling. More broadly, robust carbon accounting requires consideration of biogeochemical effects beyond the process that defines the primary CDR pathway: just

584 as enhanced weathering assessments must account for potential effects on organic carbon
585 cycling (Suhrhoff et al., 2026; Vienne et al., 2026), biochar assessments should likewise
586 account for consequences for inorganic carbon cycling. Durable biochar CDR is therefore
587 not defined by carbon persistence alone, but by the full biogeochemical consequences of
588 stabilizing that carbon including impacts on inorganic carbon cycling.

Figures

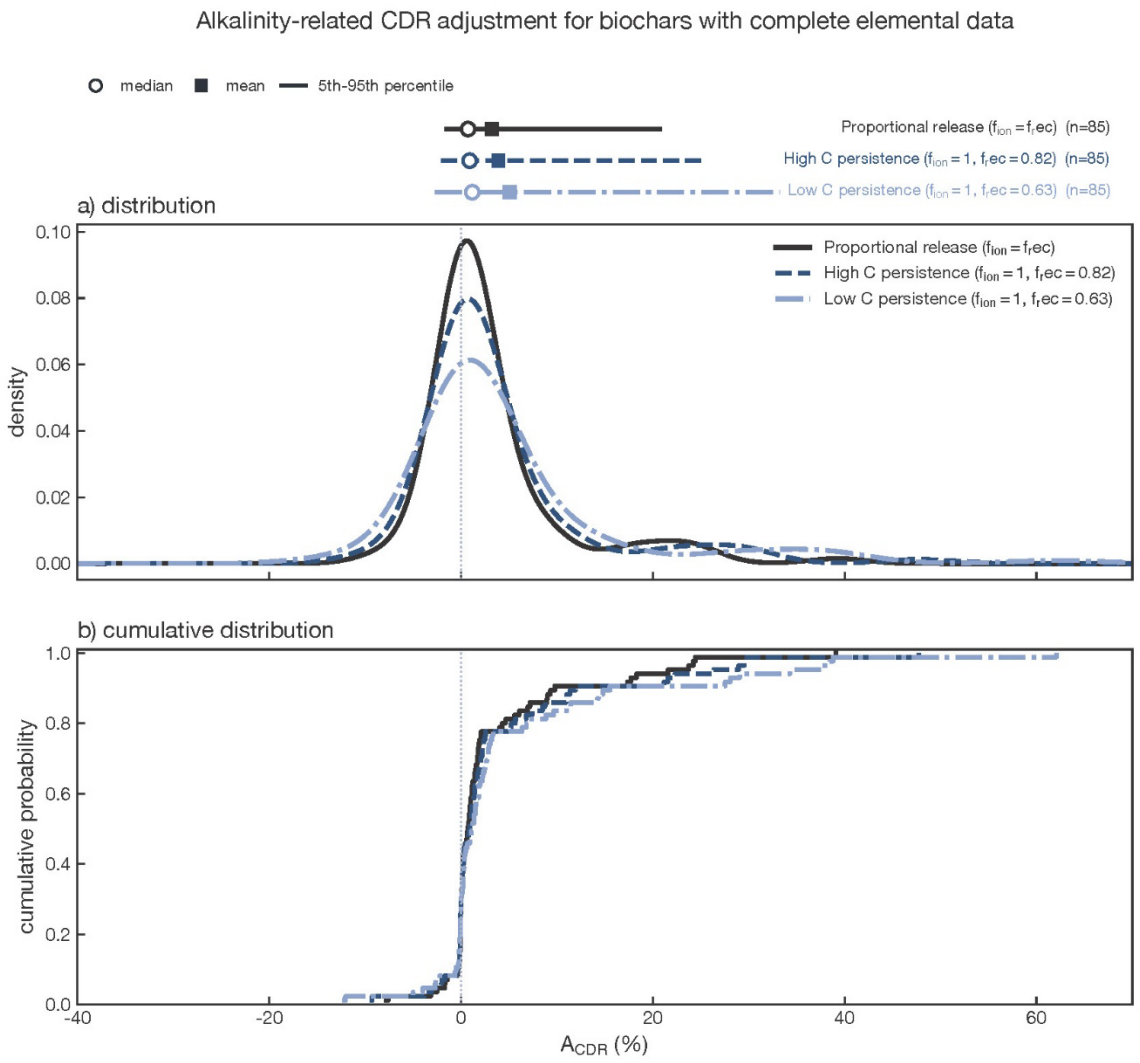

Fig. 1. Kernel density distributions (a) and cumulative frequency distributions (b) of the alkalinity-related CDR adjustment (A_{CDR}) for biochars with complete Ca, Mg, K, Na, N, and S data (n=85). Three elemental-retention scenarios are shown: proportional release ($f_{ion} = f_{rec}$), complete cation and anion elemental retention with high organic-C persistence (f_{ion}=1, f_{rec} =0.82), and complete cation and anion retention with low organic-C persistence (f_{ion}=1, f_{rec} =0.63). Mean A_{CDR} values are 3.2% ± 7.4%, 3.9% ± 9.0%, and 5.1% ± 11.7%, respectively, with corresponding medians of 0.74%, 0.91%, and 1.18%.

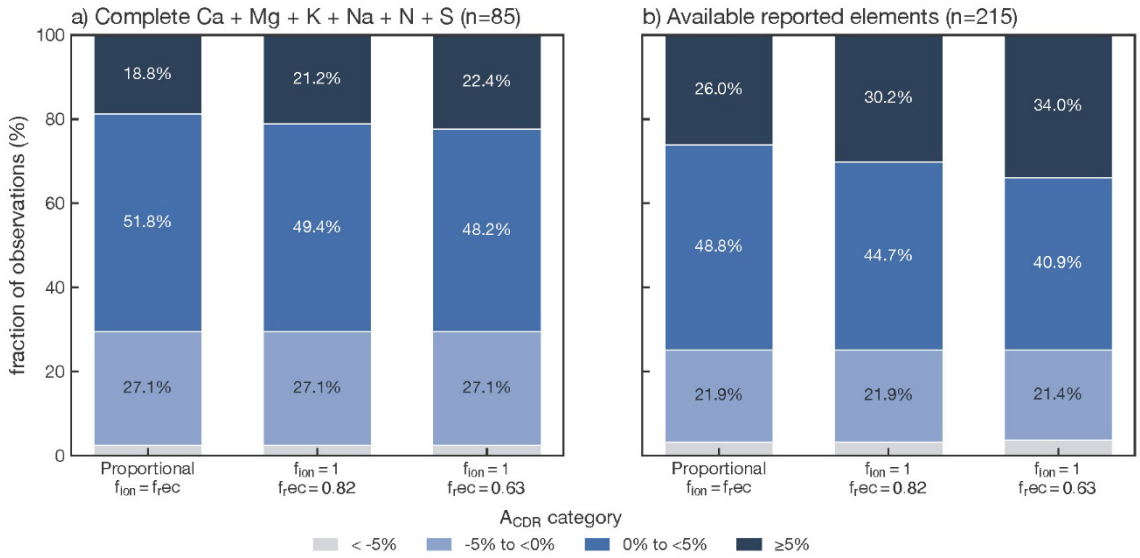

Fig. 2: Distribution of alkalinity-related CDR adjustment (A_{CDR}) categories under three elemental-retention scenarios for (a) biochars reporting complete Ca, Mg, K, Na, N, and S data (n = 85) and (b) all biochars using whatever subset of these elements was reported (n = 215). Bars show the fraction of observations with $A_{CDR} < -5\%$, $-5\% \leq A_{CDR} < 0\%$, $0\% \leq A_{CDR} < 5\%$, and $A_{CDR} \geq 5\%$. For the complete-element dataset, the fraction of observations with $A_{CDR} \geq 5\%$ was 18.8%, 21.2%, and 22.4% for proportional release ($f_{ion} = f_{rec}$), complete elemental retention with $f_{rec} = 0.82$, and complete elemental retention with $f_{rec} = 0.63$, respectively. Using all available elemental data increased these fractions to 26.0%, 30.2%, 34.0%, respectively. The larger positive adjustments in the available-element analysis partly reflect more frequent reporting of cations than anions across source studies, such that omission of unreported anion pools can bias the calculated cation–anion equivalent imbalance toward positive values.

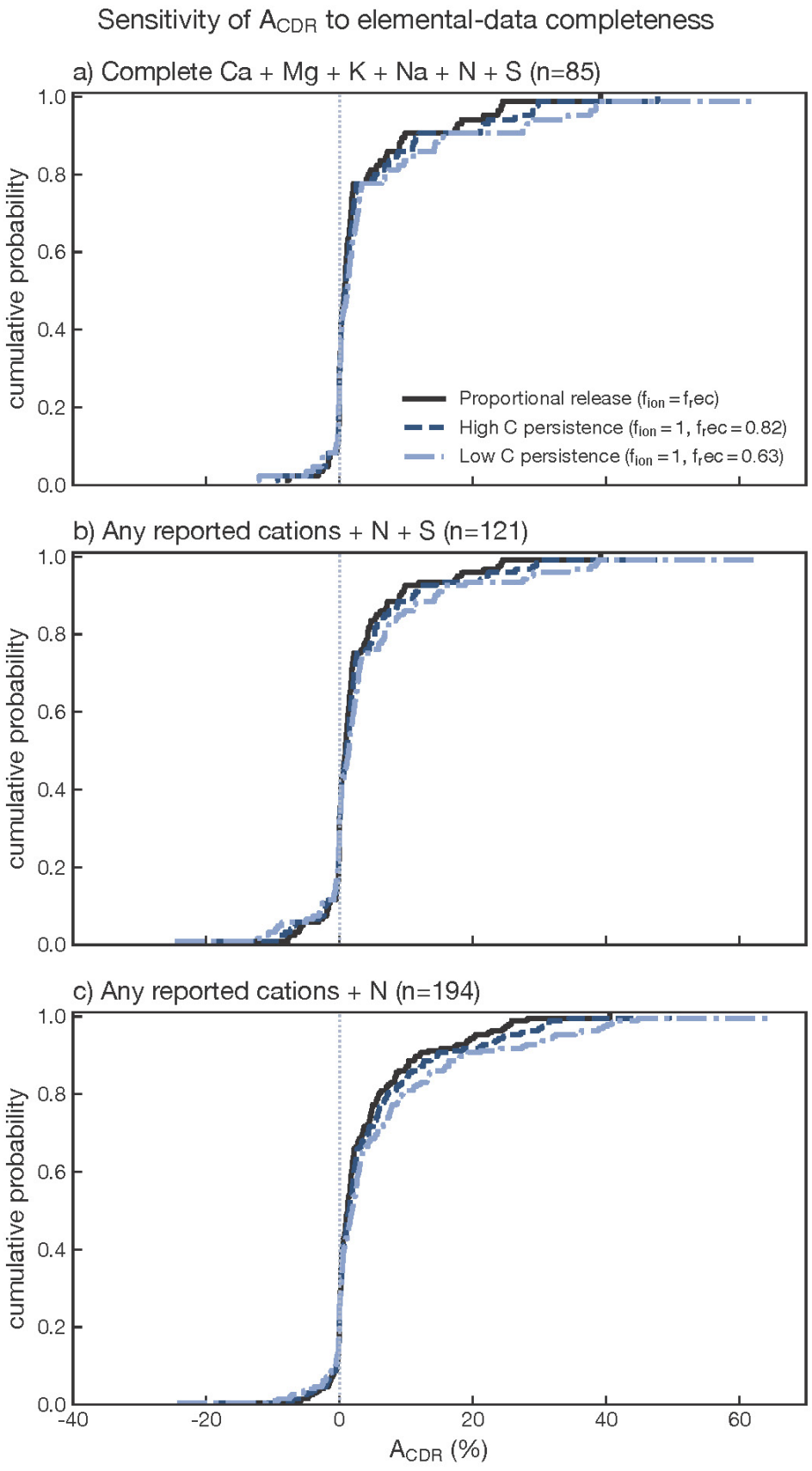
Sensitivity of A_{CDR} to elemental-data completeness
a) Complete Ca + Mg + K + Na + N + S (n=85)
b) Any reported cations + N + S (n=121)
c) Any reported cations + N (n=194)
cumulative probability
1.0
0.8
0.6
0.4
0.2
0.0
Proportional release ($f_{ion} = f_r ec$)
High C persistence ($f_{ion} = 1$, $f_r ec = 0.82$)
Low C persistence ($f_{ion} = 1$, $f_r ec = 0.63$)
-40
-20
0
20
40
60
A_{CDR} (%)

611

Fig. 3: Cumulative frequency distributions of the alkalinity-related CDR adjustment (A_{CDR}) under three elemental-retention scenarios and alternative levels of elemental-data completeness: (a) complete Ca, Mg, K, Na, N, and S data (n = 85); (b) all observations reporting N and S, with the cation-equivalent balance calculated from whichever of Ca, Mg, K, and Na were reported (n = 121); and (c) all observations reporting N, with the cation-equivalent balance calculated from whichever of Ca, Mg, K, and Na were reported (n = 194). Each panel shows proportional release ($f_{ion} = f_{rec}$), complete elemental retention with $f_{ion} = 1$ and $f_{rec} = 0.82$, and complete elemental retention with $f_{ion} = 1$ and $f_{rec} = 0.63$. Differences among panels reflect both incomplete reporting of elemental pools and differences in the biochar observations represented in each subset and therefore characterize sensitivity to elemental-data availability rather than formal uncertainty bounds.

Acknowledgments

We acknowledge funding from Yale Center for Natural Carbon Capture and the Grantham Foundation. NJP acknowledges support from Environmental Defense Fund. We furthermore thank three anonymous reviewers for their input that has improved the quality of this manuscript.

Author Contributions

All authors designed research. A.A.A. performed research. A.A.A., T.J.S., and N.J.P. analyzed data. All authors wrote the paper. All authors edited and provided feedback. A.A.A., T.J.S., & C.T.R. drafted final figures.

Conflict of Interest

Authors declare no competing interests.

Data and Supplementary Information

Biochar elemental major cation and anion content database in the form of a table is included in the supplementary information.

References

Abdel-Fattah, T. M., Mahmoud, M. E., Ahmed, S. B., Huff, M. D., Lee, J. W., & Kumar, S. (2015). Biochar from woody biomass for removing metal contaminants and carbon sequestration. *Journal of Industrial and Engineering Chemistry*, *22*, 103–109. https://doi.org/10.1016/j.jiec.2014.06.030

Alburquerque, J. A., Sánchez, M. E., Mora, M., & Barrón, V. (2016). Slow pyrolysis of relevant biomasses in the Mediterranean basin. Part 2. Char characterisation for carbon sequestration and agricultural uses. *Journal of Cleaner Production*, *120*, 191–197. https://doi.org/10.1016/j.jclepro.2014.10.080

Al-Rabaiai, A., Menezes-Blackburn, D., Al-Ismaily, S., Janke, R., Al-Alawi, A., Al-Kindi, M., & Bol, R. (2024). Biochar pH reduction using elemental sulfur and biological activation using compost or vermicompost. *Bioresource Technology*, *401*, 130707. https://doi.org/10.1016/j.biortech.2024.130707

Altıkat, A., Alma, M. H., Altıkat, A., Bilgili, M. E., & Altıkat, S. (2024). A Comprehensive Study of Biochar Yield and Quality Concerning Pyrolysis Conditions: A Multifaceted Approach. *Sustainability*, *16*(2), 937. https://doi.org/10.3390/su16020937

Al-Wabel, M. I., Al-Omran, A., El-Naggar, A. H., Nadeem, M., & Usman, A. R. A. (2013). Pyrolysis temperature induced changes in characteristics and chemical composition of biochar produced from conocarpus wastes. *Bioresource Technology*, *131*, 374–379. https://doi.org/10.1016/j.biortech.2012.12.165

Anđelini, D., Cvitan, D., Prelac, M., Pasković, I., Černe, M., Nemet, I., Major, N., Goreta Ban, S., Užila, Z., Zubin Ferri, T., Njegić Džakula, B., Petek, M., Ban, D., & Palčić, I. (2023). Biochar from Grapevine-Pruning Residues Is Affected by Grapevine Rootstock and Pyrolysis Temperature. *Sustainability*, *15*(6), 4851. https://doi.org/10.3390/su15064851

667 Anjum, R., Krakat, N., Toufiq Reza, M., & Klocke, M. (2014). Assessment of mutagenic potential
668 of pyrolysis biochars by Ames *Salmonella*/mammalian-microsomal mutagenicity test.
669 *Ecotoxicology and Environmental Safety*, *107*, 306–312.
670 https://doi.org/10.1016/j.ecoenv.2014.06.005
671 Beerling, D. J., Kantzas, E. P., Lomas, M. R., Wade, P., Eufrasio, R. M., Renforth, P., Sarkar, B.,
672 Andrews, M. G., James, R. H., Pearce, C. R., Mercure, J.-F., Pollitt, H., Holden, P. B.,
673 Edwards, N. R., Khanna, M., Koh, L., Quegan, S., Pidgeon, N. F., Janssens, I. A., …
674 Banwart, S. A. (2020). Potential for large-scale CO2 removal via enhanced rock
675 weathering with croplands. *Nature*, *583*(7815), 242–248.
676 https://doi.org/10.1038/s41586-020-2448-9
677 Bolan, N. S., Hedley, M. J., & White, R. E. (1991). Processes of soil acidification during nitrogen
678 cycling with emphasis on legume based pastures. *Plant and Soil*, *134*(1), 53–63.
679 https://doi.org/10.1007/BF00010717
680 Boraah, N., Chakma, S., & Kaushal, P. (2023). Optimum features of wood-based biochars: A
681 characterization study. *Journal of Environmental Chemical Engineering*, *11*(3), 109976.
682 https://doi.org/10.1016/j.jece.2023.109976
683 Brady, N. C., Weil, R. R., & Brady, N. C. (2010). *Elements of the nature and properties of soils*.
684 Brantley, K. E., Savin, M. C., Brye, K. R., & Longer, D. E. (2016). Nutrient availability and corn
685 growth in a poultry litter biochar-amended loam soil in a greenhouse experiment. *Soil*
686 *Use and Management*, *32*(3), 279–288. https://doi.org/10.1111/sum.12296
687 Broadley, M., Brown, P., Cakmak, I., Rengel, Z., & Zhao, F. (2012). Chapter 7 - Function of
688 Nutrients: Micronutrients. In P. Marschner (Ed.), *Marschner's Mineral Nutrition of*

689 *Higher Plants (Third Edition)* (pp. 191–248). Academic Press.
690 https://doi.org/10.1016/B978-0-12-384905-2.00007-8
691 Buss, W., Wurzer, C., Manning, D. A. C., Rohling, E. J., Borevitz, J., & Mašek, O. (2022). Mineral-
692 enriched biochar delivers enhanced nutrient recovery and carbon dioxide removal.
693 *Communications Earth & Environment*, *3*(1). https://doi.org/10.1038/s43247-022-
694 00394-w
695 Buss, W., Yeates, K., Rohling, E. J., & Borevitz, J. (2021). Enhancing natural cycles in agro-
696 ecosystems to boost plant carbon capture and soil storage. *Oxford Open Climate*
697 *Change*, *1*(1), kgab006. https://doi.org/10.1093/oxfclm/kgab006
698 Butnan, S., Deenik, J. L., Toomsan, B., Antal, M. J., & Vityakon, P. (2015). Biochar characteristics
699 and application rates affecting corn growth and properties of soils contrasting in texture
700 and mineralogy. *Geoderma*, *237–238*, 105–116.
701 https://doi.org/10.1016/j.geoderma.2014.08.010
702 Cabiyo, B., Chay, F., Field, C., Fingerman, K., Hausfather, Z., Hemes, K. S., & Zarakas, C. M. (2026).
703 Consistent temporal accounting supports credible CDR use. *CDRXIV*.
704 https://cdrxiv.org/preprint/302?version=1
705 Calabrese, S., Wild, B., Bertagni, M. B., Bourg, I. C., White, C., Aburto, F., Cipolla, G., Noto, L. V.,
706 & Porporato, A. (2022). Nano- to Global-Scale Uncertainties in Terrestrial Enhanced
707 Weathering. *Environmental Science & Technology*, *56*(22), 15261–15272.
708 https://doi.org/10.1021/acs.est.2c03163
709 Cantrell, K. B., Hunt, P. G., Uchimiya, M., Novak, J. M., & Ro, K. S. (2012). Impact of pyrolysis
710 temperature and manure source on physicochemical characteristics of biochar.
711 *Bioresource Technology*, *107*, 419–428. https://doi.org/10.1016/j.biortech.2011.11.084

CDR Leaderboards—Top Carbon Removal Suppliers, Buyers & Services | CDR.fyi. (2026). Retrieved June 12, 2026, from https://www.cdr.fyi/leaderboards

Chiaravalloti, I., Theunissen, N., Zhang, S., Wang, J., Sun, F., Ahmed, A. A., Pihlap, E., Reinhard, C. T., & Planavsky, N. J. (2023). Mitigation of soil nitrous oxide emissions during maize production with basalt amendments. *Frontiers in Climate*, *5*. https://www.frontiersin.org/articles/10.3389/fclim.2023.1203043

Clarkson, M. O., Larkin, C. S., Swoboda, P., Reershemius, T., Suhrhoff, T. J., Maesano, C. N., & Campbell, J. S. (2024). A review of measurement for quantification of carbon dioxide removal by enhanced weathering in soil. *Frontiers in Climate*, *6*, 1345224. https://doi.org/10.3389/fclim.2024.1345224

Cunningham, R. K. (1964). Cation-anion relationships in crop nutrition: III. Relationships between the ratios of sum of the cations: sum of the anions and nitrogen concentrations in several plant species. *The Journal of Agricultural Science*, *63*(1), 109–111. https://doi.org/10.1017/S0021859600015148

DeVries, T. (2022). The Ocean Carbon Cycle. *Annual Review of Environment and Resources*, *47*(Volume 47, 2022), 317–341. https://doi.org/10.1146/annurev-environ-120920-111307

De Wit, C. T., Dijkshoorn, W., Noggle, J. C. (1963). *Ionic Balance and Growth of Plants*.

Drané, M., Zbair, M., Hajjar-Garreau, S., Josien, L., Michelin, L., Bennici, S., & Limousy, L. (2024). Unveiling the Potential of Corn Cob Biochar: Analysis of Microstructure and Composition with Emphasis on Interaction with NO2. *Materials*, *17*(1), 159. https://doi.org/10.3390/ma17010159

Drever, J. I. (1988). *The geochemistry of natural waters* (Vol. 437). Prentice hall Englewood Cliffs.

735 Enders, A., Hanley, K., Whitman, T., Joseph, S., & Lehmann, J. (2012). Characterization of
736 biochars to evaluate recalcitrance and agronomic performance. *Bioresource Technology*,
737 *114*, 644–653. https://doi.org/10.1016/j.biortech.2012.03.022
738 Etter, H., Vera, A., Aggarwal, C., Delaney, M., & Manley, S. (2025). *Methodology for Biochar*
739 *Utilization in Soil and non-Soil Applications.*
740 Fernández, J. M., Nieto, M. A., López-de-Sá, E. G., Gascó, G., Méndez, A., & Plaza, C. (2014).
741 Carbon dioxide emissions from semi-arid soils amended with biochar alone or combined
742 with mineral and organic fertilizers. *Science of The Total Environment*, *482–483*, 1–7.
743 https://doi.org/10.1016/j.scitotenv.2014.02.103
744 Gao, S., DeLuca, T. H., & Cleveland, C. C. (2019). Biochar additions alter phosphorus and nitrogen
745 availability in agricultural ecosystems: A meta-analysis. *Science of The Total*
746 *Environment*, *654*, 463–472. https://doi.org/10.1016/j.scitotenv.2018.11.124
747 Gul, S., & Whalen, J. K. (2016). Biochemical cycling of nitrogen and phosphorus in biochar-
748 amended soils. *Soil Biology and Biochemistry*, *103*, 1–15.
749 https://doi.org/10.1016/j.soilbio.2016.08.001
750 Hinsinger, P., Plassard, C., Tang, C., & Jaillard, B. (2003). Origins of root-mediated pH changes in
751 the rhizosphere and their responses to environmental constraints: A review. *Plant and*
752 *Soil*, *248*(1), 43–59. https://doi.org/10.1023/A:1022371130939
753 Huang, Y., Tao, B., Lal, R., Lorenz, K., Jacinthe, P.-A., Shrestha, R. K., Bai, X., Singh, M. P., Lindsey,
754 L. E., & Ren, W. (2023). A global synthesis of biochar's sustainability in climate-smart
755 agriculture—Evidence from field and laboratory experiments. *Renewable and*
756 *Sustainable Energy Reviews*, *172*, 113042. https://doi.org/10.1016/j.rser.2022.113042

Intergovernmental Panel On Climate Change (IPCC) (Ed.). (2023). Technical Summary. In *Climate Change 2022—Mitigation of Climate Change* (1st ed., pp. 51–148). Cambridge University Press. https://doi.org/10.1017/9781009157926.002

Jahanzad, E., Barker, A. V., Hashemi, M., Eaton, T., Sadeghpour, A., & Weis, S. A. (2016). Nitrogen Release Dynamics and Decomposition of Buried and Surface Cover Crop Residues. *Agronomy Journal*, *108*(4), 1735–1741. https://doi.org/10.2134/agronj2016.01.0001

Jia, J., Li, B., Chen, Z., Xie, Z., & Xiong, Z. (2012). Effects of biochar application on vegetable production and emissions of N_2 O and CH_4. *Soil Science and Plant Nutrition*, *58*(4), 503–509. https://doi.org/10.1080/00380768.2012.686436

Joseph, S., Cowie, A. L., Van Zwieten, L., Bolan, N., Budai, A., Buss, W., Cayuela, M. L., Graber, E. R., Ippolito, J. A., Kuzyakov, Y., Luo, Y., Ok, Y. S., Palansooriya, K. N., Shepherd, J., Stephens, S., Weng, Z. (Han), & Lehmann, J. (2021). How biochar works, and when it doesn't: A review of mechanisms controlling soil and plant responses to biochar. *GCB Bioenergy*, *13*(11), 1731–1764. https://doi.org/10.1111/gcbb.12885

Kanzaki, Y., Planavsky, N. J., Zhang, S., Jordan, J., Suhrhoff, T. J., & Reinhard, C. T. (2025). Soil cation storage is a key control on the carbon removal dynamics of enhanced weathering. *Environmental Research Letters*, *20*(7), 074055. https://doi.org/10.1088/1748-9326/ade0d5

Katuwal, S., Ashworth, A., Rafsan, N.-A.-S., & Kolar, P. (2022). Characterization of Poultry Litter Biochar and Activated Biochar as a Soil Amendment for Valorization. *Biomass*, *2*(4), 209–223. https://doi.org/10.3390/biomass2040014

779 Kwoczynski, Z., Burdová, H., Al Souki, K. S., & Čmelík, J. (2024). Extracted rapeseed meal biochar
780 combined with digestate as a soil amendment: Effect on lettuce (*Lactuca sativa L.*)
781 biomass yield and concentration of bioavailable element fraction in the soil. *Scientia*
782 *Horticulturae*, *329*, 113041. https://doi.org/10.1016/j.scienta.2024.113041
783 Lataf, A., Jozefczak, M., Vandecasteele, B., Viaene, J., Schreurs, S., Carleer, R., Yperman, J.,
784 Marchal, W., Cuypers, A., & Vandamme, D. (2022). The effect of pyrolysis temperature
785 and feedstock on biochar agronomic properties. *Journal of Analytical and Applied*
786 *Pyrolysis*, *168*, 105728. https://doi.org/10.1016/j.jaap.2022.105728
787 Lefebvre, D., Fawzy, S., Aquije, C. A., Osman, A. I., Draper, K. T., & Trabold, T. A. (2023). Biomass
788 residue to carbon dioxide removal: Quantifying the global impact of biochar. *Biochar*,
789 *5*(1), 65. https://doi.org/10.1007/s42773-023-00258-2
790 Lehmann, J., Cowie, A., Masiello, C. A., Kammann, C., Woolf, D., Amonette, J. E., Cayuela, M. L.,
791 Camps-Arbestain, M., & Whitman, T. (2021). Biochar in climate change mitigation.
792 *Nature Geoscience*, *14*(12), 883–892. https://doi.org/10.1038/s41561-021-00852-8
793 Li, H., Lu, X., Xu, Y., & Liu, H. (2019). How close is artificial biochar aging to natural biochar aging
794 in fields? A meta-analysis. *Geoderma*, *352*, 96–103.
795 https://doi.org/10.1016/j.geoderma.2019.06.006
796 Li, S. (2024). Reviewing Air Pollutants Generated during the Pyrolysis of Solid Waste for Biofuel
797 and Biochar Production: Toward Cleaner Production Practices. *Sustainability*, *16*(3),
798 1169. https://doi.org/10.3390/su16031169
799 Li, S., & Shangguan, Z. (2018). Positive effects of apple branch biochar on wheat yield only
800 appear at a low application rate, regardless of nitrogen and water conditions. *Journal of*
801 *Soils and Sediments*, *18*, 3235–3243.

802 Macdonald, L. M., Farrell, M., Zwieten, L. V., & Krull, E. S. (2014). Plant growth responses to
803 biochar addition: An Australian soils perspective. *Biology and Fertility of Soils*, *50*(7),
804 1035–1045.
805 Marschner, H. (2011). *Marschner's Mineral Nutrition of Higher Plants*. Academic Press.
806 Menegat, S., Ledo, A., & Tirado, R. (2022). Greenhouse gas emissions from global production
807 and use of nitrogen synthetic fertilisers in agriculture. *Scientific Reports*, *12*(1), 14490.
808 https://doi.org/10.1038/s41598-022-18773-w
809 Meyer zu Drewer, J., Vorrath, M.-E., Amann, T., Hartmann, J., Ansari, M., Cárcamo Pérez, M., &
810 Hagemann, N. (2026). Combining biochar and basanite rock powder enhances carbon
811 dioxide removal by carbonate alkalinity production. *Frontiers in Climate*, *8*.
812 https://doi.org/10.3389/fclim.2026.1853116
813 Mohanty, P., Nanda, S., Pant, K. K., Naik, S., Kozinski, J. A., & Dalai, A. K. (2013). Evaluation of the
814 physiochemical development of biochars obtained from pyrolysis of wheat straw,
815 timothy grass and pinewood: Effects of heating rate. *Journal of Analytical and Applied*
816 *Pyrolysis*, *104*, 485–493. https://doi.org/10.1016/j.jaap.2013.05.022
817 Naeem, M. A., Khalid, M., Arshad, M., & Ahmad, R. (2014). *YIELD AND NUTRIENT COMPOSITION*
818 *OF BIOCHAR PRODUCED FROM DIFFERENT FEEDSTOCKS AT VARYING PYROLYTIC*
819 *TEMPERATURES*.
820 Nan, H., Yin, J., Yang, F., Luo, Y., Zhao, L., & Cao, X. (2021). Pyrolysis temperature-dependent
821 carbon retention and stability of biochar with participation of calcium: Implications to
822 carbon sequestration. *Environmental Pollution*, *287*, 117566.
823 https://doi.org/10.1016/j.envpol.2021.117566

824 Nordahl, S. L., Hanes, R. J., Mayfield, K. K., Myers, C., Baker, S. E., & Scown, C. D. (2024). Carbon
825 accounting for carbon dioxide removal. *One Earth*, *7*(9), 1494–1500.
826 Novak, J. M., Cantrell, K. B., & Watts, D. W. (2013). Compositional and Thermal Evaluation of
827 Lignocellulosic and Poultry Litter Chars via High and Low Temperature Pyrolysis: High
828 and Low Temperature Pyrolyzed Biochars. *BioEnergy Research*, *6*(1), 114–130.
829 https://doi.org/10.1007/s12155-012-9228-9
830 Noyce, G., Jones, T., Fulthorpe, R., & Basiliko, N. (2017). Phosphorus uptake and availability and
831 short-term seedling growth in three Ontario soils amended with ash and biochar.
832 *Canadian Journal of Soil Science*, CJSS-2017-0007. https://doi.org/10.1139/CJSS-2017-
833 0007
834 Nwajiaku, I. M., Olanrewaju, J. S., Sato, K., Tokunari, T., Kitano, S., & Masunaga, T. (2018).
835 Change in nutrient composition of biochar from rice husk and sugarcane bagasse at
836 varying pyrolytic temperatures. *International Journal of Recycling of Organic Waste in*
837 *Agriculture*, *7*(4), 269–276. https://doi.org/10.1007/s40093-018-0213-y
838 Obey, G., Adelaide, M., & Ramaraj, R. (2022). Biochar derived from non-customized matamba
839 fruit shell as an adsorbent for wastewater treatment. *Journal of Bioresources and*
840 *Bioproducts*, *7*(2), 109–115. https://doi.org/10.1016/j.jobab.2021.12.001
841 Omotade, İ., Momoh, S., Oluwafemi, B., & Agboola, E. (2020). Comparative analysis of nutrients
842 composition in biochar produced from different feedstocks at varying pyrolysis
843 temperature. *Environmental Research and Technology*, *3*(2), 64–70.
844 https://doi.org/10.35208/ert.747833
845 Qadir, M. F., Naveed, M., Khan, K. S., Mumtaz, T., Raza, T., Mohy-Ud-Din, W., & Mustafa, A.
846 (2024). Divergent responses of phosphorus solubilizing bacteria with P-laden biochar for

enhancing nutrient recovery, growth, and yield of canola (*Brassica napus* L.). *Chemosphere*, *353*, 141565. https://doi.org/10.1016/j.chemosphere.2024.141565

Redin, M., Recous, S., Aita, C., Dietrich, G., Skolaude, A. C., Ludke, W. H., Schmatz, R., & Giacomini, S. J. (2014). How the chemical composition and heterogeneity of crop residue mixtures decomposing at the soil surface affects C and N mineralization. *Soil Biology and Biochemistry*, *78*, 65–75. https://doi.org/10.1016/j.soilbio.2014.07.014

Schimmelpfennig, S., & Glaser, B. (2012). One Step Forward toward Characterization: Some Important Material Properties to Distinguish Biochars. *Journal of Environmental Quality*, *41*(4), 1001–1013. https://doi.org/10.2134/jeq2011.0146

Singh, B., Singh, B. P., & Cowie, A. L. (2010). Characterisation and evaluation of biochars for their application as a soil amendment. *Soil Research*, *48*(7), 516–525.

Sohng, J., Sokol, N. W., Whiteaker, S., Schmidt, R., Holzer, I., Goertzen, H., Peña, J., Houlton, B. Z., Montañez, I., O'Geen, A., & Scow, K. (2025). Combining organic amendments with enhanced rock weathering shifts soil carbon storage in croplands. *Science of The Total Environment*, *998*, 180179. https://doi.org/10.1016/j.scitotenv.2025.180179

Sparling, G. P., McLay, C. D. A., Tang, C., & Raphael, C. (1999). Effect of short-term legume residue decomposition on soil acidity. *Australian Journal of Soil Research*, *37*(3), 561–574. https://doi.org/10.1071/S98104

Subedi, R., Taupe, N., Pelissetti, S., Petruzzelli, L., Bertora, C., Leahy, J. J., & Grignani, C. (2016). Greenhouse gas emissions and soil properties following amendment with manure-derived biochars: Influence of pyrolysis temperature and feedstock type. *Journal of Environmental Management*, *166*, 73–83. https://doi.org/10.1016/j.jenvman.2015.10.007

Suhrhoff, T. J., Dietzen, C., Kukla, T., Lunstrum, A., Reershemius, T., Thompson, J. T., Almaraz, M., Bertagni, M. B., Bullock, L. A., & D'Ascanio, R. (2026). An Ecosystem of Carbon Dioxide Removal Reviews–Part 3: Enhanced Weathering. *CDRXIV*. https://cdrxiv.org/preprint/417?version=1

Suhrhoff, T. J., Reinhard, C., Kanzaki, Y., Tsao, S. S.-E., Woollen, B., Reershemius, T., Shaheen, S., Saiers, J., Zhang, S., Raymond, P., & Planavsky, N. (2026). *Agricultural liming is a large carbon sink in the Mississippi River Basin*. Research Square. https://doi.org/10.21203/rs.3.rs-7068561/v1

Tang, C., & Rengel, Z. (2003). Role of Plant Cation/Anion Uptake Ratio in Soil Acidification. In *Handbook of Soil Acidity*. CRC Press.

Tepecik, M., Ekren, S., Ongun, A. R., & Sarikahya, N. B. (2024). Effects of biochar treatments on the elemental composition of tobacco (Nicotiana tabacum L.) leaves based on the priming period. *Heliyon*, *10*(1), e23307. https://doi.org/10.1016/j.heliyon.2023.e23307

Usman, A. R. A., Abduljabbar, A., Vithanage, M., Ok, Y. S., Ahmad, M., Ahmad, M., Elfaki, J., Abdulazeem, S. S., & Al-Wabel, M. I. (2015). Biochar production from date palm waste: Charring temperature induced changes in composition and surface chemistry. *Journal of Analytical and Applied Pyrolysis*, *115*, 392–400. https://doi.org/10.1016/j.jaap.2015.08.016

Van Zwieten, L., Kammann, C., Cayuela, M. L., Singh, B. P., Joseph, S., Kimber, S., Donne, S., Clough, T., & Spokas, K. A. (2015). Biochar effects on nitrous oxide and methane emissions from soil. In *Biochar for environmental management* (pp. 489–520). Routledge.

892 Vienne, A., Cox, T., Niron, H., Guenet, B., Poetra, R., Steinwidder, L., Vandenhove, C., & Vicca, S.
893 (2026). Integrating Experiments and Models To Unravel Interactions between Soil
894 Organic Matter and Enhanced Weathering. *Environmental Science & Technology*, *60*(27),
895 19249–19261. https://doi.org/10.1021/acs.est.6c00236
896 Waheed, A., Xu, Q., Cui, D., Muhammad, M., Xu, H., Aili, A., Kuerban, A., & Ali, S. (2026). Biochar
897 as a climate-smart strategy for restoring dryland soils and mitigating desertification.
898 *Biochar*, *8*(1), 59. https://doi.org/10.1007/s42773-025-00537-0
899 Walling, E., & Vaneeckhaute, C. (2020). Greenhouse gas emissions from inorganic and organic
900 fertilizer production and use: A review of emission factors and their variability. *Journal*
901 *of Environmental Management*, *276*, 111211.
902 https://doi.org/10.1016/j.jenvman.2020.111211
903 Wang, J., Xiong, Z., & Kuzyakov, Y. (2016). Biochar stability in soil: Meta-analysis of
904 decomposition and priming effects. *GCB Bioenergy*, *8*(3), 512–523.
905 https://doi.org/10.1111/gcbb.12266
906 Wang, K., Peng, N., Lu, G., & Dang, Z. (2020). Effects of Pyrolysis Temperature and Holding Time
907 on Physicochemical Properties of Swine-Manure-Derived Biochar. *Waste and Biomass*
908 *Valorization*, *11*(2), 613–624. https://doi.org/10.1007/s12649-018-0435-2
909 Wang, L., O'Connor, D., Rinklebe, J., Ok, Y. S., Tsang, D. C. W., Shen, Z., & Hou, D. (2020). Biochar
910 Aging: Mechanisms, Physicochemical Changes, Assessment, And Implications for Field
911 Applications. *Environmental Science & Technology*, *54*(23), 14797–14814.
912 https://doi.org/10.1021/acs.est.0c04033

Wang, Y., Hu, Y., Zhao, X., Wang, S., & Xing, G. (2013). Comparisons of biochar properties from wood material and crop residues at different temperatures and residence times. *Energy & Fuels*, *27*(10), 5890–5899.

Williams, J. M., & Thomas, S. C. (2023). High-carbon wood ash biochar for mine tailings restoration: A field assessment of planted tree performance and metals uptake. *Science of The Total Environment*, *901*, 165861. https://doi.org/10.1016/j.scitotenv.2023.165861

Woolf, D., Lehmann, J., Ogle, S., Kishimoto-Mo, A. W., McConkey, B., & Baldock, J. (2021). Greenhouse Gas Inventory Model for Biochar Additions to Soil. *Environmental Science & Technology*, *55*(21), 14795–14805. https://doi.org/10.1021/acs.est.1c02425

Wrobel-Tobiszewska, A., Boersma, M., Sargison, J., Adams, P., & Jarick, S. (2015). An economic analysis of biochar production using residues from Eucalypt plantations. *Biomass and Bioenergy*, *81*, 177–182. https://doi.org/10.1016/j.biombioe.2015.06.015

Wu, C., Coffield, S. R., Goulden, M. L., Randerson, J. T., Trugman, A. T., & Anderegg, W. R. L. (2023). Uncertainty in US forest carbon storage potential due to climate risks. *Nature Geoscience*, *16*(5), 422–429. https://doi.org/10.1038/s41561-023-01166-7

Xiao, R., Wang, J. J., Gaston, L. A., Zhou, B., Park, J.-H., Li, R., Dodla, S. K., & Zhang, Z. (2018). Biochar produced from mineral salt-impregnated chicken manure: Fertility properties and potential for carbon sequestration. *Waste Management*, *78*, 802–810. https://doi.org/10.1016/j.wasman.2018.06.047

Xu, X., Zhao, Y., Sima, J., Zhao, L., Mašek, O., & Cao, X. (2017). Indispensable role of biochar-inherent mineral constituents in its environmental applications: A review. *Bioresource Technology*, *241*, 887–899. https://doi.org/10.1016/j.biortech.2017.06.023

936 Yang, J., Zhao, Z., Hu, Y., Abbey, Lord, Cesarino, I., Goonetilleke, A., & He, Q. (2023). Exploring
937 the Properties and Potential Uses of Biocarbon from Spent Coffee Grounds: A
938 Comparative Look at Dry and Wet Processing Methods. *Processes*, *11*(7), Article 7.
939 https://doi.org/10.3390/pr11072099
940 Zeebe, R. E., & Wolf-Gladrow, D. (2001). *CO2 in Seawater: Equilibrium, Kinetics, Isotopes*. Gulf
941 Professional Publishing.
942 Zhang, Q., Song, Y., Wu, Z., Yan, X., Gunina, A., Kuzyakov, Y., & Xiong, Z. (2020). Effects of six-
943 year biochar amendment on soil aggregation, crop growth, and nitrogen and
944 phosphorus use efficiencies in a rice-wheat rotation. *Journal of Cleaner Production*, *242*,
945 118435. https://doi.org/10.1016/j.jclepro.2019.118435
946 ZHAO, X., Dan, L., Juan, K., & LIN, Q. (2014). Does biochar addition influence the change points
947 of soil phosphorus leaching? *Journal of Integrative Agriculture*, *13*(3), 499–506.
948 Zhao, Y., Zhao, L., Mei, Y., Li, F., & Cao, X. (2018). Release of nutrients and heavy metals from
949 biochar-amended soil under environmentally relevant conditions. *Environmental Science*
950 *and Pollution Research*, *25*, 2517–2527.
951